POST-LAUNCH ANALYSIS

William Eustace, Euan Baines, Yuki de Pourbaix, Alex Forey, Hugo Cheema-Grubb, James Crompton, Igor Timofeev, Neel Le Penru

Abstract: Team Impulse produced a rover for the European CanSat competition which successfully recorded and sent back to the ground internal temperature, pressure and humidity. The altitude calculations based on pressure data were especially interesting, since they showed a reduction in descent speed which, it is suggested, was caused by the increase in air density on descent and thermals rising from the warm ground below. A brief description of the rover, both mechanically and electronically, is given, along with the lessons learnt from the project in terms of mechanical and electronic design. The rover, although it was not demonstrated immediately after launch, was tested and demonstrated to the judges the day after launch; the circumstances contributing to this failure are described.

Figure 1--CanSat before launch

I. INTRODUCTION

A CanSat is a simulation of a satellite mission in which the satellite must fit inside the form factor of a drinks can: a cylinder 115mm in length by 66mm in diameter. This presents certain engineering constraints in the design of mechanical, electronic and structural components. Team Impulse elected to produce a rover which would attempt to move across the ground after landing. It was also intended to measure temperature, pressure, and humidity, while also producing an infrared heat map of the ground below.

II PROJECT DESCRIPTION

The design chosen for the rover used two wheels (one at each end), and had a strut for stabilisation, which was deployed using a spring. There was also a mechanism for releasing the parachute after landing, which was tested successfully.

Electronically, the core of the design was a customised printed circuit board (PCB), with a temperature and humidity sensor, magnetometer, and GPS mounted off board. These data were relayed back over an ultra-high frequency (UHF) radio link.

II.I Materials and structural design

The CanSat main chassis was manufactured from acrylic and aluminium. The structure involved an aluminium shell and base plate, with an acrylic structure internally to hold the motors, electronics and parachute release mechanism. MDF modesty blocks were used to support the motors. The wheels were made of acrylic with an aluminium back-plate to ensure that the impact of landing would not shatter them. Figure 1 shows a photograph of the rover, with the parachute attached, shortly before launch. To improve repeatability and reliability, the design was produced using CAD software; Figure 2 shows the CAD model.

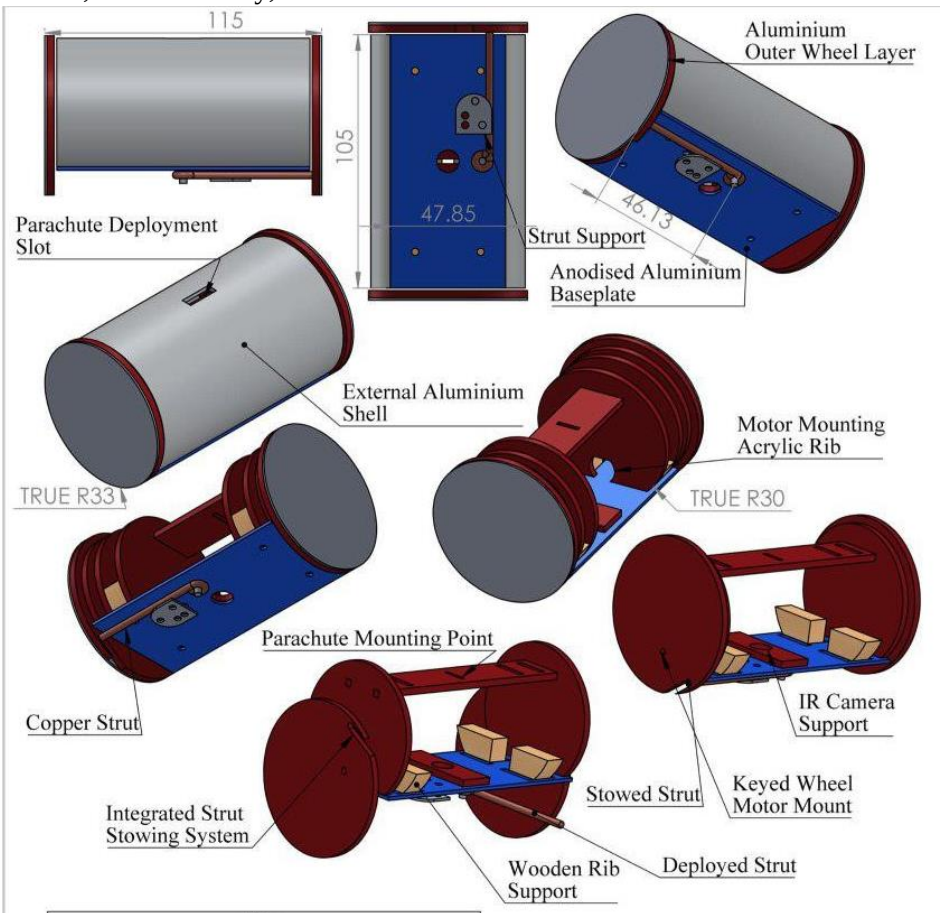

Key	
Colour	**Material**
Grey	Aluminium
Red	Acrylic
Blue	Anodised Aluminium
Brown	Copper
Wood Texture	MDF

Figure 2 - CAD model

II.II Manufacture

The acrylic components were laser cut. The aluminium shell was cut by hand on a bandsaw. The MDF components were laser cut. The base-plate aluminium sheet shape and cut-outs were laser scored onto a piece of anodised aluminium, then cut using a guillotine; in the case of the round IR camera cut-out, it was drilled and then filed to shape.

II.III Electronics

The electronics design was produced using CAD (RS DesignSpark PCB) and sent for manufacture by PCBTrain, a sponsor of the project. The design consisted of a single printed circuit board (Figure 3 shows both sides) which was assembled by hand.

II.IV Software & Firmware

The rover's firmware was developed in a modular fashion, in which several libraries were produced for peripherals before the main body of code was written. The software on the base station presented a graphical user interface for control of the rover in addition to pre-processing and logging the data. (N.B. pre-processing refers here to the process of bit-shifting the data from the raw bytes in which it is sent/received into integers/floats as appropriate.)

III SCIENTIFIC RESULTS

The following graphs were obtained of temperature, pressure and humidity. From these were extrapolated graphs of height above launch altitude (hereafter height) and dew point, by equations [1] and [2] respectively.

$$dp(T,RH) = \frac{\lambda\left(\ln\frac{RH}{100} + \frac{\beta\cdot T}{\lambda+T}\right)}{\beta - \left(\ln\frac{RH}{100} + \frac{\beta\cdot T}{\lambda+T}\right)} \quad [1]$$

In [1], $dp(T,RH)$ gives the dew point in degrees Celsius: T is the temperature, RH is the relative humidity, λ and β are constants, and $\ln x$ refers to the natural logarithm of x.

$$ht(P,QFE) = \left(1 - \left(\frac{P}{QFE}\right)^{\alpha}\right) \times \beta \quad [2]$$

In [2], $ht(P,QFE)$ gives the height above the level of the ground at which QFE is measured in feet; P is the pressure in millibars, QFE is the pressure at ground level (QFE is widely used in light aviation in Britain, but QNH (pressure at mean sea level) is more commonly used on the continent). α and β are constants.

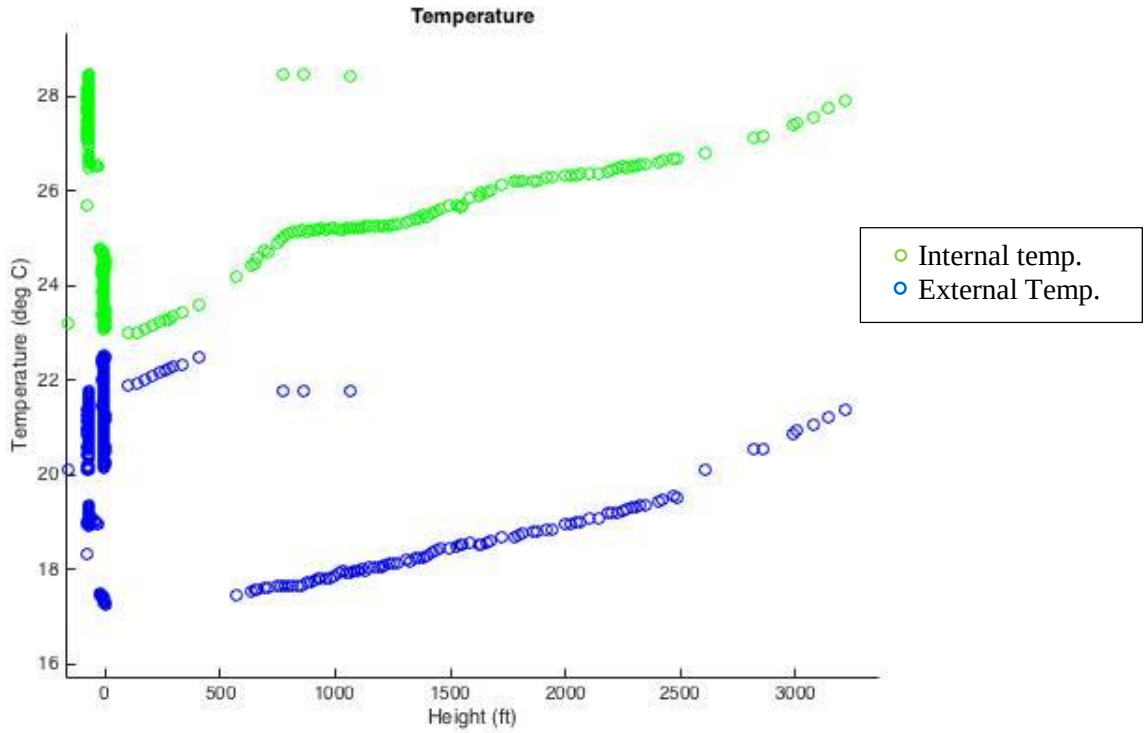

Figure 3 - Temperature graph

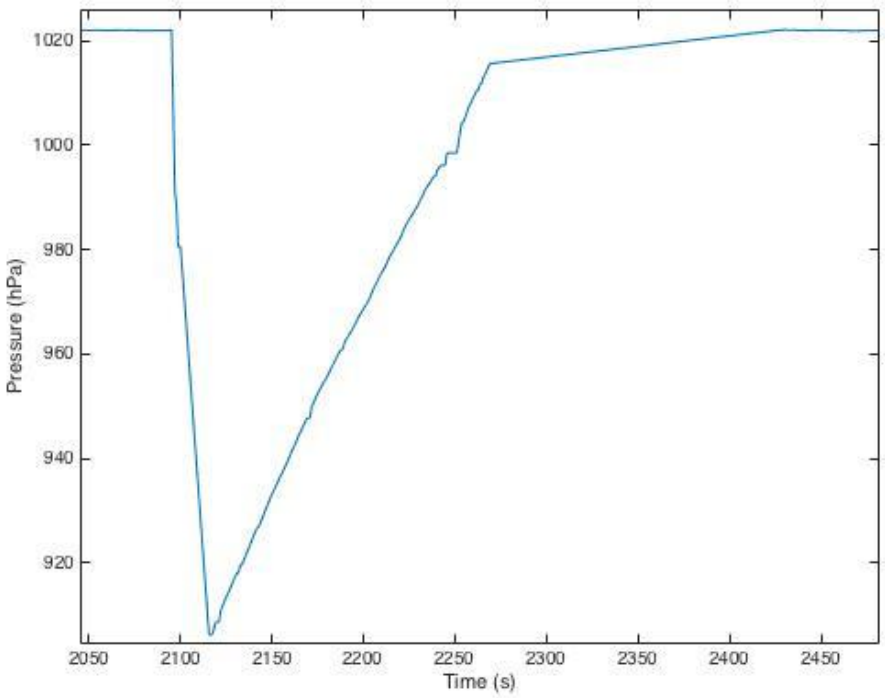

Figure 4 - Pressure graph

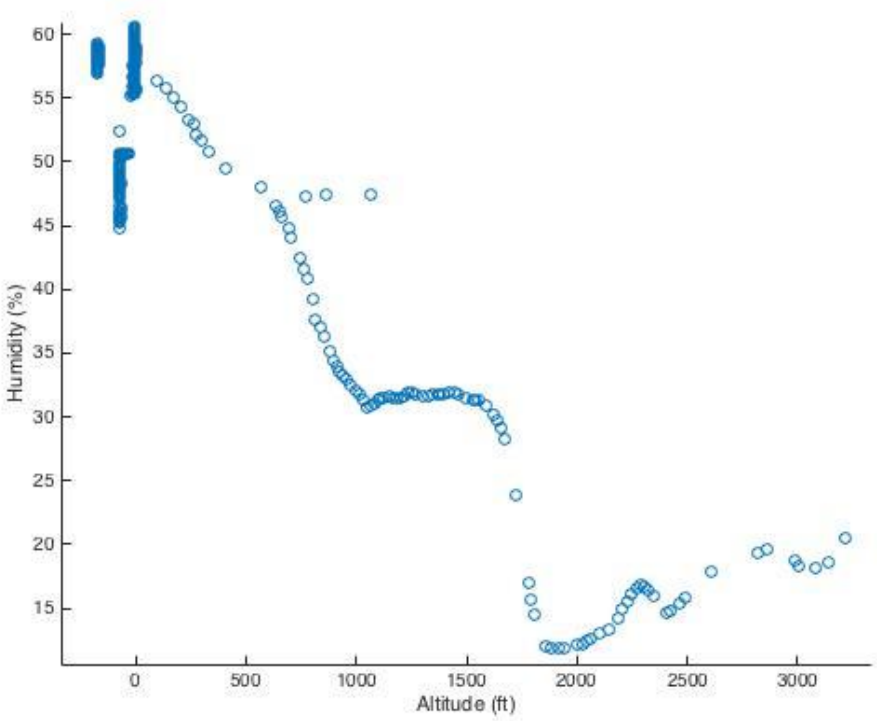

Figure 6 - Humidity graph

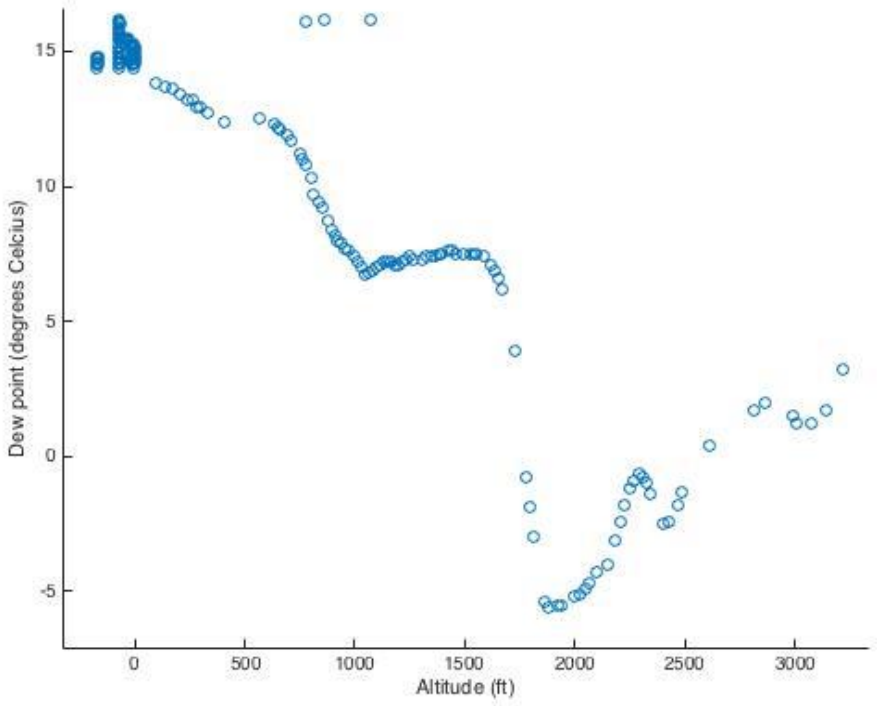

Figure 5 - Dew Point graph

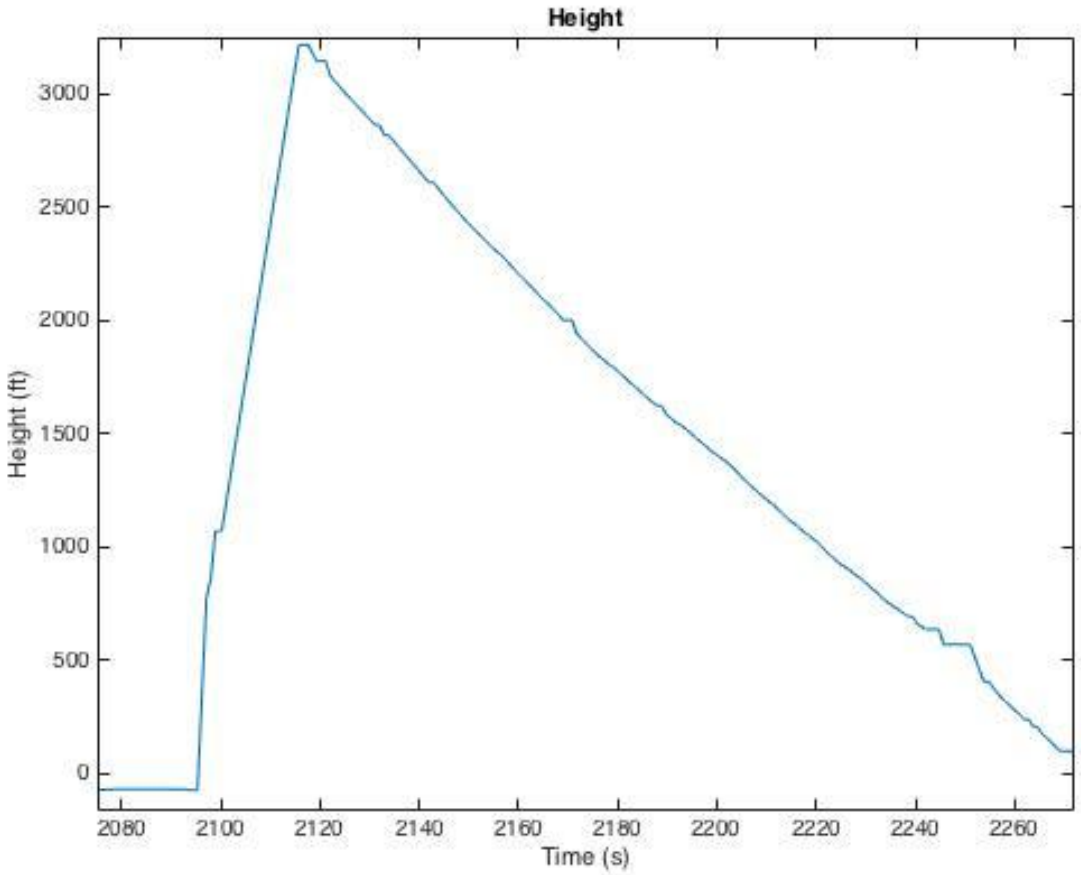

Figure 8 - Height graph

Finally, an infra-red (IR) camera was to be used in tandem with a magnetometer and GPS to generate a heat-map of the ground below. Regrettably the IR camera developed a mechanical defect the night before launch and so was not flown; however, a sample heat-map is included for discussion.

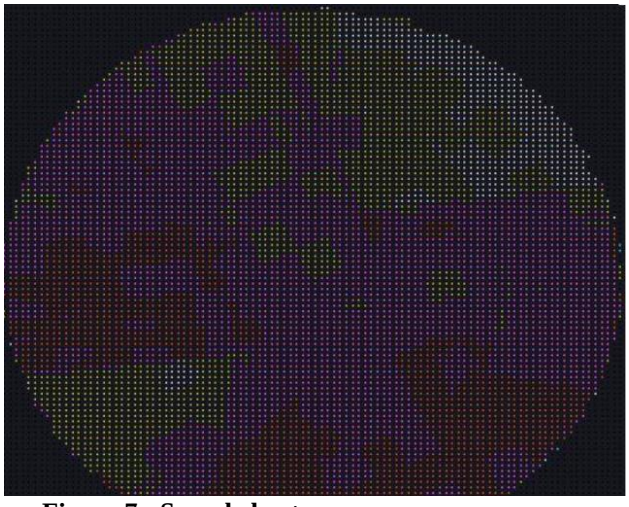

Figure 7 - Sample heat map

IV DISCUSSION

The temperature graph (Fig 3) shows internal and external temperature. The internal temperature is shown in green, and is markedly warmer than the external temperature; this is due to the different placement of the sensors. The internal temperature sensor is on the main PCB, and so allows measurement of the heat produced by the electronics. The external temperature probe is mounted just inside an aperture in the can which allows air circulation. There was a temperature inversion in effect on the day of the launch (as confirmed by airport staff) which was responsible for the increase in temperature with altitude (rather than the decrease one would expect). There is a distinct correlation between the graphs, however; this indicates that the external temperature sensor was not completely in equilibrium with the outside air; a possible improvement would be to have the sensor protruding from the can entirely. The three anomalous points between 500 and 1,000 feet are likely data points collected during the ascent of the can—there were very few of these since a data rate of around 1Hz was used and the rocket's ascent took less than 10s. They may be explained either by the propagation of heat from the rocket motor upwards (considered relatively unlikely) or the effect of a lack of air circulation on the contents of the rocket, with electronics heating. The alternative explanation is an error in data transmission, but this is considered unlikely due to the mode of action of the LoRa modem. Overall, though, the temperature measurement may be considered a success.

The pressure/time graph shows, much as one would expect, a rapid decrease from ground level pressure of approximately 1022 hPa to a little over 900 hPa; this decrease is as one would expect for an altitude of 1000m. The failure of the graph to return to its previous level is explained by the loss of radio connection on the CanSat dropping below the horizon. The pressure measurement is successful in its primary aim—to determine the CanSat's altitude.

The humidity/height graph is worthy of further analysis, since it shows quite clearly the presence of various vapour layers on the descent. The general decrease in humidity with altitude is as one would expect; the plateaus and gradient changes show vapour layers. There may be some inaccuracy in the shape of the graph owing to the aforementioned coupling of the external temperature sensor (which was on the same module as the hygrometer) to the air mass inside the can. Despite this, however, the humidity measurement gave a result much as might have been expected, so can be considered successful.

Figure 9 - Weather on launch day

The dew point, as calculated in equation [1], shows a heavy correlation with humidity, as would be expected; the high level of variance leads to the conclusion that dew point measured at ground level may not always be accurate at altitude. This presents hazards for pilots, especially of light aircraft—icing of wings, propellers, and, in the case of aircraft of older design (including most of the current light aircraft fleet), carburettor icing. The calculated dew point remained significantly below the measured air temperature at all times, which would agree with the fact that no cloud cover was observable on the day of launch over the launch site (see Fig 9). The dew point calculation, notwithstanding the slight

concerns of poor air circulation around the hygrometer, may be considered successful.

The graph of altitude with time is much as one would expect; the initial ascent is completed in approximately 20 seconds to an apogee of 3290 ft above the ground. This is followed by a slower-than-expected descent, at approximately 6m/s, to the ground. This is within the 20% tolerance applied to the competition descent rate requirements and so may be considered successful.

In order to make a closer analysis of the descent rate, a line was plotted against it. This makes it clear that the rate of descent was not constant.

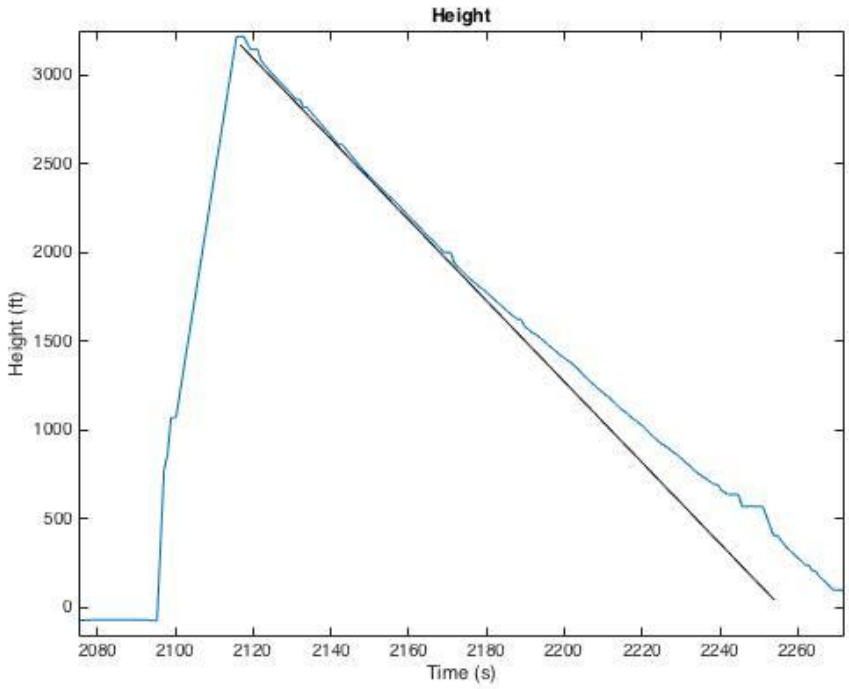

Figure 10 - Altitude graph with descent line

The change in the descent rate is quite significant, moving from about 6 m/s to about 3-4 m/s. This is ascribed mainly to the change in air density, which one would expect.

$$\rho = \frac{pM}{RT} \quad [3]$$

In equation [3], a formula for density is presented which takes into account the pressure, the molecular mass of the air, and the air temperature. The following change in conditions is taken to have occurred:

Table 1 - Density changes

	Ground	Apogee
Pressure (Pa)	102,200	90,600
Temperature (K)	288	292
Density (kg m^{-3})	1.24	1.08

The following equation gives the expected terminal velocity of a parachute and payload:

$$V_t = \sqrt{\frac{2mg}{\rho A C_d}} \quad [4]$$

In equation [4], V_t represents the terminal velocity, m the mass, g the acceleration due to gravity, ρ the air density, A the reference area of the parachute, and C_d the drag coefficient. Rewriting it to separate the density and absorb $\frac{2mg}{AC_d}$ into a single constant,κ, yields equation [5]:

$$V_t = \sqrt{\rho^{-1} \times \kappa} \quad [5]$$

Applying equation [5] yields the following extension of Table 1, using a value for κ calculated to fit an initial descent rate (as observed) of 7.3 m/s:

Table 2 - Expected terminal velocities

	Ground	Apogee
Predicted terminal velocity (m/s)	6.8	7.3

This is significantly less of a reduction than actually observed (final measured descent rate was approx. 5.5 m/s). This disparity from expected descent rate may likely be explained by circulation of thermals from the fields below; these are believed to be responsible for the irregularities visible in the altitude graph as the can reached altitudes below 1000ft.

That it is possible to infer such fine details from the data collected suggests that the altitude collection part of the project was especially successful.

The heat-map sample included was taken during earlier testing of the sensor from a height of approx. 4 m. The sensor, fitted with magnetometer, was held above the border between grass and paving, a line to the north-west of the camera. The sensor and magnetometer were rotated through a complete circle twice, held in the same location, and the resultant data run through the heat-map generation script. The result is Fig. 7; the dividing line between the grass and the paving can clearly be seen—the paving retains more heat than the grass and so is shown in a darker shade. Although this indicates that, were it flown, this project would have been successful, the lack of flight data confirmation makes it impossible to be confident.

V ROVER

The rover itself was unable to be demonstrated immediately after landing for three core reasons: the radio link (used for telecommand) was severed as the CanSat fell below the horizon; the wheels of the CanSat detached on landing due to inadequate bonding between the wheels and the motor shafts; and the CanSat was recovered before the parachute release command had been received.

After recovery, with no software or hardware modifications whatsoever, the CanSat telecommand system was tested and found functional. The parachute release mechanism worked and the motor shafts turned as commanded. The autonomous navigation system could not be tested owing to the wheel failures.

The wheels were reattached in preparation for the presentation to the judges the next day; the CanSat was then reassembled and demonstrated successfully before the judges.

VI CONCLUSION

During the launch, there was no opportunity to test the IR camera or rover functionalities, owing to failures in system components; however, data were successfully streamed back live to the ground and logged. These data were analysed and found broadly in accordance with expectations. Internal temperature, external temperature, pressure, and humidity were successfully monitored; there are some concerns about the ties between the thermal mass of the can and the external temperature sensor which should be addressed for future missions of this sort. The rover was not successfully demonstrated during the launch but was shown to function during the presentations. Future projects using a similar design must pay special attention to the strength of the join between the wheels and the motor shafts or axles, if used. The structure of an acrylic tray for electronics sliding into an aluminium shell was efficient, but access to electronics (especially batteries) must be made as easy as possible. Electronics designers intending to use Lithium-Ion or Lithium-Polymer batteries in the CanSat competition would be well advised to use, as this project did, a battery with a built-in over-discharge prevention circuit, which has a great positive effect on safety. On one occasion during the build programme, the system was accidentally left on for a period exceeding 8 hours; the cut-off functioned as expected and subsequent analysis suggested the cut-off to have occurred at the nominal 2.7 V.